Angular Dependence of DRAM Upset Susceptibility and Implications for Testing and Analysis

Steven M. Guertin, *Member, IEEE*, Larry D. Edmonds, and Gary M. Swift, *Member IEEE*

***Abstract*--Heavy ion irradiations of two types of commercial DRAMs reveal unexpected angular responses. One device's cross section varied by two orders of magnitude with azimuthal angle. Accurate prediction of space rates requires accommodating this effect.**

I. Introduction

The upset responses of various dynamic random access memories (DRAMs) have been studied previously, as they are becoming more prevalent in space missions [1-5]. Many different types of responses have been seen in these devices, including single-bit upset, bit-line upset [6], single event functionality interrupt (SEFI), and stuck bits [7]. This paper investigates two angular dependencies of single-bit upset response to heavy ions in some typical DRAMs.

The usual way of testing devices involves hitting the device with multiple ion species and energies using several tilt angles, θ (angles relative to normal incidence), to increase effective LET. The ideal test matrix would include many ion species and energies at normal incidence. Because of accelerator facility and test cost limitations, upset data is usually taken for only a few ions at several tilt angles and is interpreted, as far as possible, using the "cosine law" for LET

$$LET_{effective} = LET_{incident} / \cos\theta . \qquad (1)$$

The cosine law also multiplies the directional cross section (defined as the number of events divided by beam fluence) by $\sec\theta$ to obtain the area in the device plane whose projection in the beam direction is the measured cross section. The cosine law originated from the concept of a thin sensitive volume (SV), but is not expected to apply to very large angles (approaching 90°) for two reasons. The first reason is that an SV thickness small enough for the cosine law to apply to the smaller angles may still not be small enough for the cosine law to apply to larger angles. The second reason is that, even if the cosine law did apply to the very penetrating particles found in space, it may still not apply to test data obtained from affordable (moderate energy) facilities, because of ion range limitations. Regardless of whether the cosine law or some other law (e.g., corrections suggested by Petersen [8]) will be used, ion range limitations and other difficulties in obtaining very steep tilt angles [9] limit the tilt angles that can be used. In practice, tilt angles only up to about 60° are used to measure upset cross sections. In space, ions are omnidirectional. The solid angle between normal incidence and 60°, front and back, is only half of the total. Upset rate calculations are lacking experimental data at large angles, so the correct angular response must be incorporated into the rate calculation via modeling. The best that can be done is to confirm that the tilt angle response used in the rate calculation agrees with the highest angle results in the data set.

The above discussion was concerned with tilt angles. There can also be azimuth angle dependencies. Upset data collection and rate calculations typically ignore this. The accuracy of the space upset rate calculations depends on assuming either (a) there is no azimuthal dependence or (b) the data is a reasonable average over all azimuthal angles.

Azimuth and tilt angle dependencies were experimentally explored for two DRAMs to identify whether the behavior was consistent with traditional assumptions. An unexpectedly large azimuthal dependence was found in one of the test device types. The other device was found to be nearly isotropic, but non-traditional plots were needed to reveal this behavior (traditional plots are badly scattered).

Data were taken using several ions at various tilt angles, as well as various azimuthal angles. For several fixed tilt angles between 0° and 66°, the devices were rotated in small steps over 360° of azimuth. Two device types, Oki MSM514400 4Mb DRAMs and Toshiba TC5165805AFT-50 64Mb DRAMs, were chosen; the former representative of current in-

Manuscript received July 26, 2000. The research in this paper was carried out by the Jet Propulsion Laboratory, California Institute of Technology, under contract with the National Aeronautics and Space Administration. It was sponsored by the NASA Electronic Parts and Packaging Program (Code AE).

The authors are with the Jet Propulsion Laboratory, California Institute of Technology, Pasadena, California, USA, 91109.

flight devices on JPL spacecraft and the latter representative of newer generation DRAMs.

II. MBUs

DRAMs are typically susceptible to multiple-bit-upsets (MBUs), i.e., one particle hit upsets several bits or cells. This discussion excludes those cases (e.g., SEFI or bit-line upsets) in which upsets or transients in one device structure is the cause of upsets in other components, so the focus is on the more conventional type of MBU investigated by Zoutendyk *et al*. [10]. The SV model has trouble explaining the MBU phenomenon. An attempt to explain MBU from normal-incident heavy ions via the SV model assumes that SVs for different cells overlap. But this implies that several cells each collect all of the charge liberated in the overlapping region, so this attempted explanation is unrealistic. In contrast, MBU is easily explained in terms of charge sharing by different cells [11]. Some fraction of the liberated charge is collected by one cell, and another fraction is collected by another cell. Charge collected by a given cell is well defined in this model for any heavy-ion hit location, even if the ion hits another cell. This makes an individual cell cross section for a given heavy ion well defined, in terms of the hit locations that will upset that cell. Individual cell cross sections increase with increasing ion LET, and can sometimes become large enough to overlap. Hits to overlap regions produce MBUs.

Several types of device cross sections can be defined. One type, called the U-type here (U for upset), is calculated from the total number of upsets observed during an SEU test, while another type, called the G-type here (G for group), counts the number of occurrences of upset groups. An upset group is defined here to be the set of upsets (one or more) produced by the same particle hit. For example, if one particle hit upsets four cells, the U-type cross section counts this as four upsets, while the G-type counts this as one group. The G-type is useful when one upset group is regarded as one device failure, regardless of whether the group contains one or many cell upsets. However, only the U-type device cross section has the property of being the sum of the bit or cell cross sections. If all cells in the device are identical, the cell (or bit) cross section is the U-type device cross section divided by the number of cells in the device. Therefore, the cross section for a single cell is determined by measuring the U-type device cross section. The cross section for a single cell is important for SEU rate calculations because DRAMs used in flight applications are typically protected by EDAC (because the SEU rate would be unacceptable otherwise). For EDAC to be effective, the device architecture is arranged so that multiple cell upsets created by a single particle hit are in different EDAC words, so an uncorrectable error (two or more cell upsets within a common word and during a common scrub time) requires multiple particle hits. Calculating uncorrected error rates then requires a calculation of the rate of occurrence of two or more statistically independent cell upsets within a common word and during a common scrub time, hence upset rates for individual cells are relevant. Because this information is derived from U-type device cross sections, all device cross sections reported here are U-type.

For the benefit of those readers that are (for whatever reason) interested in G-type cross sections, multiplicity factors (which are divided into the U-type cross sections to produce G-type) are presented for the Oki device in Fig. 1. Ratios have not been determined for the Toshiba device because the required logical to physical device map is not known for that device. Without that mapping, it is guesswork to determine when G-type events cause multiple U-type events.

Note that after the G-type device cross section saturates to the entire device area (every ion hit upsets at least one cell), the U-type will continue to increase with LET if the multiplicity factor continues to increase. In general, an increase in the U-type device cross section with LET directly measures an increase in a cell cross section. An increase in the multiplicity factor is also related (but the measure is not as simple in general) to an increase in the cell cross section, because a larger cell cross section implies that it overlaps a larger number of other cell cross sections.

III. TEST METHODOLOGY

Testing was conducted using a special DRAM test board, and custom-built PCI-to-digital I/O board which allows testing of DRAMs at 160,000 addresses per second. The OKI devices were obtained from the Cassini flight lot, which were purchased as die and hermetically packaged. They required only lid and polyaimide removal as preparation for heavy ion testing. The Toshiba devices were commercial plastic-encapsulated parts that were completely disassembled and re-bonded for testing in order to eliminate interference from the lead frame.

Testing was done at Brookhaven National Laboratory with seven ion species: 56.3MeV lithium, 97.5MeV carbon, 141MeV fluorine, 186MeV silicon, 210MeV chlorine, 229MeV titanium, and 266MeV nickel. The range of normal incident nickel ions was 42.4 μ m and is the shortest of the selection. The devices were tested with a data pattern, known as “inverse bleed down,” in which all bits were susceptible to upset.

(By exposing a DRAM die to a normal white light bulb for several minutes, the charge on the memory cells is drained-off enough to look like no charge is present (to the sense amps). This state of the device’s cells is called the “bleed down” pattern, and is not susceptible to single-bit-upsets. The bit-wise inverse of this pattern is the “inverse bleed down” pattern.)

Measures were taken to eliminate upsets such as bit-line upset or SEFI. Runs were discarded if the number of bit upsets was much larger than the number of addresses that those bits were in. Stucks were also an issue, and where possible were subtracted from the total number of bit upsets.

IV. Results

A. Oki DRAM Results

When tilted along various azimuthal angles, the Oki devices showed too little azimuthal dependence to be of concern. Because of this, cross sections for the Okis were averaged over azimuthal angles. These data are plotted in the traditional format (i.e., converted via the cosine law) in Fig. 2. Note that the data are badly scattered, indicating cosine law failure. The ions at normal incidence are left hollow so that they can be distinguished from the other points.

B. Toshiba DRAM Results

The Toshiba's angular response is more complicated than the Oki's. We observed an extreme variation in cross section with azimuthal angle for the lower LET ions at moderate tilt angles. Fig. 3 shows an example where the device was struck with fluorine at a 48 tilt angle along azimuthal angles in increments of 15 . Note the factor of ~100 difference between 0 (or 180) and 90 (or 360). Other tilt angles and other low LET ions also show the response is strongly dependent on azimuthal angle.

It is illustrative to consider the different results that would be obtained if tests were done at only one azimuthal angle. Fig. 4 and Fig. 5 show cross section versus LET data taken at two azimuthal angles (as indicated in the insets – one along the long-axis (0°) the other along the short-axis (90°). From Fig. 4, one would conclude that (1) is working well and miscalculate the GCR upset rate by over a factor of 10 since the major difference is in the low LET region. Fig. 5 signals a tilt-angle problem. Note the similarity to Fig. 2; however, removing the "cosine" dependence, as was done in Fig. 6 (discussed later), does not collapse Fig. 5 to a smooth function. Either orientation results in serious SEU rate error.

V. Theory

A theoretical analysis in the appendix shows how data for the OKI device can be plotted to more clearly reveal a trend. The analysis concludes that a plot of directional cross section (not cross section times $\sec\theta$) versus ion LET (not LET times $\sec\theta$) becomes nearly independent of θ (i.e., device susceptibility becomes nearly isotropic) at sufficiently large LET. The analysis does not answer the question of how large "sufficiently large" is, but it does inspire us to re-plot the OKI data by removing the secants from both the cross section and LET. The result is shown in Fig. 6, which is much less scattered than Fig. 2. For this particular device, the figure shows that the susceptibility is roughly isotropic for all LET. This type of plot does not help with the Toshiba, because "sufficiently large LET" is the largest LET used in the test, so the device is not isotropic for LET in most of the plotted range. Additional work is needed to theoretically predict the best way to plot data for devices such as this one.

An analysis that is related to the one we used (appendix) to predict the directional dependencies was previously presented by Smith et al. [12]. The equation that applies to the physical conditions assumed in our appendix is their equation (3) (note that their σ is the A in our appendix, which is the σ in our appendix divided by $\cos\theta$). However, in order for the σ in their equation to be the SEU cross section, the q (a charge fluence) in their equation must be an "effective" value. In fact, their equation (3) is the definition of this effective value for the physical conditions that the equation is intended for. It is therefore not clear what directional dependencies are implied by this equation, because the effective q may depend on θ . The authors did not address this, so we used the alternate analysis in the appendix. Incidentally, our analysis shows that their q does depend on θ , but is approximately independent of θ when the ion LET is large.

We have not attempted to fit the data using the HICUP model [13], although we suspect that it probably will fit because of its many adjustable parameters. However, given that the model does *fit* the data, it still does not *explain* the data, because the physical assumptions are inappropriate. One assumption is the RPP model, which is clearly inappropriate for DRAMs, because charge can be collected from remote locations (as evidenced by MBUs at normal incidence). Another assumption is that the variation of cross section with increasing LET is from a statistical distribution of critical charges. It was known for some time, and recently acknowledged in [14], that variation in the cross section is largely, if not almost entirely, the result of collected charge varying with hit location (again contradicting the RPP model). It might be assumed that the directional dependencies for this situation are the same as for a collection of geometrically identical RPPs with statistically distributed critical charges, but the validity of this assumption is not self evident. It might be speculated that the RPP model describes charge collection during early times. This originates from a common belief that charge collection at early times is almost exclusively by drift, with diffusion becoming important only at later times. However, this unfounded assertion is not supported by analysis of the transport equations [15,16]. Even computer simulation results, which have been interpreted as supporting this assertion, present numbers without explanations, so the identification of a current as "drift" is the investigator's interpretation. Furthermore, a simple inspection of the spacing between equipotential surfaces shows that regions that have been identified as "funnels" from simulation results are not strong-field drift regions; they are weak-field ambipolar diffusion regions [15,16]. A careful analysis of the drift-diffusion equations [15,16] found that diffusion is always important at all times. The RPP model is not physically realistic, but enough adjustable parameters (including a funnel length selected as needed to improve the fit) can fit data without the model being valid. Model validity is more of a concern when the objective is not merely to fit

existing data, but rather to extrapolate data from moderate-range ions and moderate tilt angles in the laboratory to long-range ions and large angles in space. Therefore, there is still a motivation to look for physically correct models. The analysis by Smith et al. [12], and the analysis in the appendix of the present paper, might be of some assistance to future work in this area.

VI. A Comparison Between Rate Predictions

Models that are approximately compatible with the approximately isotropic behavior for the OKI include a perfectly isotropic device, and a collection of rectangular parallelepipeds (RPPs) that are cubes. A collection of RPPs having an aspect ratio (A) (lateral dimension divided by thickness) of 5 are not consistent with the OKI data, but this model does approximate the angular dependencies for many other devices, so we will call it a "typical" RPP. It is interesting to compare SEU rates calculated from each model. The perfectly isotropic model calculates rates by simply integrating the omnidirectional flux with the device cross section curve. The second and third models use an IRPP calculation, but with A=1 and A=5, respectively. Another model included in the comparison assumes that the cosine law is valid up to 85°, but excludes ions at larger angles. The rates in interplanetary space (or geosynchronous orbit) are compared in Table I. The comparison shows that failure to take enough data to recognize the tilt angle dependence changes the calculated rate significantly (also note the isotropic and cube RPP rates differ by only 4%).

VII. Conclusion

In order to calculate realistic space upset rates, one must make additional measurements to investigate azimuthal angle effects. In particular, for unusual tilt angle dependencies, more testing is needed to obtain the same quality cross section versus LET information than would be required if the cosine law applied. Azimuthal dependencies should be checked at LET's near threshold using 0° (or 180°) and 270° (or 90°) for fixed tilt. If found, a large data set is required, at least until a community-accepted model of the azimuthal dependence is developed.

These results show that the angular response of DRAM upsets can be more complicated than previously thought. The large azimuthal response has not been reported previously. It is important to measure, in detail, how the upset susceptibility varies with tilt angle and, at least, to check the assumption of azimuthal angle invariance. Devices like the 64Mb Toshiba DRAMs, which violate that assumption, require detailed measurements of at least one quadrant (0-90°) of azimuth angle.

For the Oki device, only the tilt angle dependence needed careful consideration. The cosine law fails because this device was found to be nearly isotropic at all LETs, which is also consistent with no azimuthal dependence. The appendix predicts this effect at sufficiently large LET (though it does not say what "sufficiently large" is).

DRAMs are unique only in the sense that the integration time for the charge to diffuse does not matter (DRAM refresh intervals are very long), and the only observable cell information is a reading of "1" or "0." Though the material discussed is applicable to other device types, it is uncertain how great the effect could be because, for most other devices, integration time is important.

VIII. Appendix: A Theoretical Prediction

A theoretical prediction of the large-LET behavior of the SEU cross section is derived from physical assumptions that are believed to be adequate approximations for DRAMs. One assumption is that an SEU occurs in a selected DRAM cell if the total (integrated in time from zero to infinity) charge collected by the cell from an ion track exceeds some critical value. Another physical assumption is that charge transport in a DRAM is primarily by diffusion. Charge collection under these conditions can be described by a charge collection efficiency function Ω, which is a function of the spatial coordinates within the device. For a given point x in the device, $\Omega(x)$ is defined to be the fraction of any charge liberated near the point x that is collected by the selected cell. It was previously shown that, for the physical assumptions stated above, Ω satisfies Laplace's equation [11]. Charge sharing by other cells is built into Ω via boundary conditions. Specifically, Ω corresponding to the selected cell is zero at any point in the device such that all charge liberated at that point is collected by some other cell. A cell is mathematically modeled as a region in the upper device plane. Let the selected cell be denoted C_0 (a set of points in the x,y plane) and let some other cell, the ith cell, be denoted C_i (another set of points in the x,y plane). The coordinate system is oriented so that the device interior is described by z>0. The boundary value problem governing Ω is

$$\nabla^2 \Omega(x,y,z) = 0 \quad if\ z > 0$$
$$\Omega(x,y,0) = 1 \quad if\ (x,y) \in C_0$$
$$\Omega(x,y,0) = 0 \quad if\ (x,y) \in C_i \quad for\ some\ i \neq 0$$

with reflective boundary conditions assumed at reflective boundaries. This boundary value problem will be approximated by another problem. Consider a point x in the upper device plane (z=0) that is many cells away from the selected cell C_0. Virtually no charge liberated at this point x will be able to get past the other cells in order to reach the selected cell, so $\Omega \approx 0$ at x. This is not the same as saying that charge will not travel great distances to reach the selected cell when liberated far *below* the point x (which is far away from other cells), so we do not use $\Omega \approx 0$ for other points at the same lateral location but greater depths. We use the approximation when x is far from the selected cell and is

also in the upper device plane so that it is near other cells, i.e., the approximation is an approximation for boundary conditions. Using this approximation, the boundary value problem becomes

$$\nabla^2\,\Omega(x,y,z)=0 \quad if\ z>0$$
$$\Omega(x,y,0)>0 \quad if\ (x,y)\in S$$
$$\Omega(x,y,0)=0 \quad if\ (x,y)\notin S$$

for some region S in the x,y plane, which contains C_0. The solution for z>0 is

$$\Omega(x,y,z)=$$
$$\frac{z}{2\pi}\int_S \frac{\Omega(x',y',0)}{[(x-x')^2+(y-y')^2+z^2]^{3/2}}\,dx'\,dy' \quad (z>0). \quad (A1)$$

An ion track is described by an LET L, a direction represented by a unit vector $\hat{n}$, and a hit location given by the lateral coordinates x,y where the ion intersects the upper device plane. Let $Q(x,y;L,\hat{n})$ denote the charge collected by the selected cell from such a track. The directional cross section, denoted $\sigma(L,\hat{n})$, for LET L and direction $\hat{n}$, is given by

$$\sigma(L,\hat{n})=\cos\theta\ A(L,\hat{n}) \quad (0\le\theta<\pi/2) \qquad (A2)$$

where θ is the angle between $\hat{n}$ and the device normal, and $A(L,\hat{n})$ is the area in the device plane of the set of points x,y such that hits to these points, by ions with LET L and direction $\hat{n}$, produce upsets. (Some mathematical difficulties can be avoided by insisting that $0\le\theta<\pi/2$.) Upsets are produced when $Q(x,y;L,\hat{n})$ exceeds the critical charge, denoted Q_C, so

$$A(L,\hat{n})=\left[\begin{array}{l} area\ enclosed\ by\ the\ curve \\ consisting\ of\ the\ points\ x,y \\ satisfying\quad Q(x,y;L,\hat{n})=Q_C \end{array}\right]. \quad (A3)$$

To calculate the area in (A3), note that Q can be expressed in terms of a line integral of Ω according to

$$Q(x,y;L,\hat{n})=a\,L\int_0^\infty \Omega(x+n_x t,\ y+n_y t,\ n_z t)\,dt$$

where n_x, n_y, and n_z are the components of $\hat{n}$, and a is a unit conversion factor for converting LET into liberated charge per unit length along the track. Substituting (A1) into the above equation and integrating in t gives

$$Q(x,y;L,\hat{n})=$$
$$\int_S \frac{(1/2\pi)\,a\,L\cos\theta\,\Omega(x',y',0)}{(x-x')n_x+(y-y')n_y+\sqrt{(x-x')^2+(y-y')^2}}\,dx'\,dy'.$$

The mean value theorem for integrals allows us to write this as

$$Q(x,y;L,\hat{n})=$$
$$\frac{\frac{1}{2\pi}\,a\,L\cos\theta\int_S \Omega(x',y',0)\,dx'\,dy'}{(x-x^*)n_x+(y-y^*)n_y+\sqrt{(x-x^*)^2+(y-y^*)^2}} \quad (A4)$$

for some appropriate $(x^*,y^*)\in S$. For notational brevity, x^* and y^* are not shown as functions of x, y, n_x, and n_y, but they do depend on these parameters.

To obtain the large-L approximation, note that a point (*x,y*) satisfying (A3) is on the cross section perimeter. For sufficiently large L, such points will be far outside of the set S. When (*x,y*) is far outside the set S, and (*x*,y**) is in S, the right side of (A5) is not sensitive to the exact location of (*x*,y**). Let the coordinate system be translated so that the origin is a point in S. Then we have the approximation

$$Q(x,y;L,\hat{n})\approx\frac{C\,L\cos\theta}{x\,n_x+y\,n_y+\sqrt{x^2+y^2}}$$
(when x,y satisfies (A3) and L is sufficiently large)

where C is a constant defined by

$$C\equiv\frac{a}{2\pi}\int_S \Omega(x',y',0)\,dx'\,dy'.$$

The large-L approximation for (A3) becomes

$$x\,n_x+y\,n_y+\sqrt{x^2+y^2}=\frac{C}{Q_C}L\cos\theta$$
$$(large-L\ approximation\ for\ (A3)). \quad (A5)$$

The curve defined by (A5) is easier to recognize in a rotated coordinate system. Let ϕ be the azimuthal angle for $\hat{n}$ so that

$$n_x=\sin\theta\cos\phi,\quad n_y=\sin\theta\sin\phi,\quad n_z=\cos\theta$$

and define the rotated coordinates ξ_1 and ξ_2 by

$$x=\xi_1\cos\phi-\xi_2\sin\phi,\quad y=\xi_1\sin\phi+\xi_2\cos\phi$$

so (A5) can be written as

$$\left(\frac{Q_C\cos\theta}{C\,L}\right)^2\left[\xi_1+\frac{C}{Q_C}L\tan\theta\right]^2+\left(\frac{Q_C}{C\,L}\right)^2\xi_2{}^2=1.$$

This equation describes an ellipse with major axis equal to $2CL/(Q_C\cos\theta)$ and minor axis equal to $2CL/Q_C$. The enclosed area, which is $A(L,\hat{n})$, is $\pi C^2L^2/(Q_C{}^2\cos\theta)$, so (A2) gives

$$\sigma(L,\hat{n})=\frac{\pi\,C^2\,L^2}{Q_C{}^2}\quad(\textit{large L approximation}).\quad(A6)$$

Note that the right side of (A6) does not depend on either angle θ or ϕ, i.e., the directional cross section becomes isotropic in the large-L limit.

IX. References

[1] R. Harboe-Sørenson, M. Brüggemann, R. Müller, F.J. Rombeck, "Radiation Evaluation of 3.3 Volt 16 M-bit DRAMs for Solid State Mass Memory Space Application," 1998 IEEE Radiation Effects Data Workshop, pp. 74-79.

[2] P. Layton, H. Anthony, R. Boss, P. Hsu, "Radiation Testing Results of COTS Based Space Microcircuits," 1998 IEEE Radiation Effects Data Workshop, pp. 170-176.

[3] K.A. LaBel, A.K. Moran, C.M. Seidleck, E.G. Stassinopoulos, J.M. Barth, P.M. Marshall, M.Carts, C. Marshall, J. Kinneson, "Single Event Test Results for Candidate Spacecraft Electronics," 1997 IEEE Radiation Effects Data Workshop, pp. 14-21.

[4] B. Doucin, C. Poivey, C. Carlotti, A. Salminen, K. Ojasalo, R. Ahonen, P. Poirot, L. Baudry, and R. Har-boe-Sørenson, "Study of Radiation Effects on Low Voltage Memories," RADECS'97 Proceedings, pp. 561-9.

[5] K.A. LaBel, M.M. Gates, A.K. Moran, H.S. Kim, C.M. Seidleck, P. Marshall, J. Kinison, "Radiation Effect Characterization and Test Methods of Single-Chip and Multi-Chip Stacked 16Mbit DRAMs," IEEE Trans. Nucl. Sci., 43, pp.2043-2048, Dec. 1996.

[6] L.W. Massengill, "Cosmic and Terrestrial Single-Event Radiation Effects in Dynamic Random Access Memories" IEEE Trans. Nucl. Sci., 43, pp. 576-593, Apr. 1996.

[7] G.M. Swift, D.J. Padgett, and A.H. Johnston, "A New Class of Hard Errors," IEEE Trans. Nucl. Sci., 41, pp.2043-2048, Dec. 1994.

[8] E.L. Petersen, J.C. Pickel, E.C. Smith, P.J. Rudeck, and J.R. Letaw, "Geometrical Factors in SEE Rate Calculations," IEEE Trans. Nucl. Sci., 40, pp. 1888-1909, Dec. 1993.

[9] O. Messeau et al., "Analysis of Multiple Bit Upsets (MBU) in a CMOS SRAM," IEEE Trans. Nucl. Sci., 43, pp. 2879-2888, Dec. 1996.

[10] J.A. Zoutendyk, L.D. Edmonds, and L.S. Smith, "Characterization of Multiple-Bit Errors from Single-Ion Tracks in Integrated Circuits," IEEE Trans. Nucl. Sci., 36, pp. 2267-2274, Dec 1989.

[11] L.D. Edmonds, "A Graphical Method for Estimating Charge Collected by Diffusion from an Ion Track," IEEE Trans. Nucl. Sci., 43, pp. 2346-2357, Aug. 1996.

[12] E.C. Smith, E.G. Stassinopoulos, K. LaBel, G. Brucker, and C.M. Seidlick, "Application of a Diffusion Model to SEE Cross Sections of Modern Devices," IEEE Trans. Nucl. Sci., 42, pp. 1772-1779, Dec. 1995.

[13] L.W. Connell, F.W. Sexton, and A.K. Prinja, "Further Development of the Heavy Ion Cross Section for Single Event Upset: Model (HICUP)," IEEE Trans. Nucl. Sci., 42, pp. 2026-2034, Dec. 1995.

[14] E.L. Petersen, "Cross Section Measurements and Upset Rate Calculations," IEEE Trans. Nucl. Sci., 43, pp. 2805-2813, Dec. 1996.

[15] L.D. Edmonds, "Charge Collection from Ion Tracks in Simple EPI Diodes," IEEE Trans. Nucl. Sci., 44, pp. 1448-1463, June 1997.

[16] L.D. Edmonds, "Electric Currents Through Ion Tracks in Silicon Devices," IEEE Trans. Nucl. Sci., 45, pp. 3153-3164, Dec. 1998.

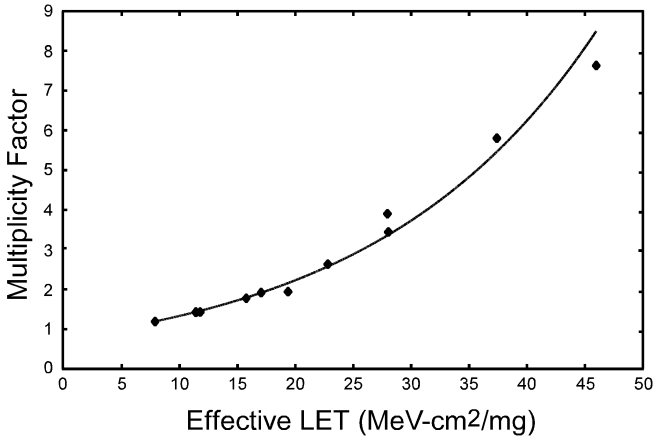

Fig. 1. The relationship between U type and G type upsets on the Oki device. This analysis requires knowledge of a device's logical to physical address translation. The authors do not have that information for the Toshiba, so similar analysis cannot be done for that device.

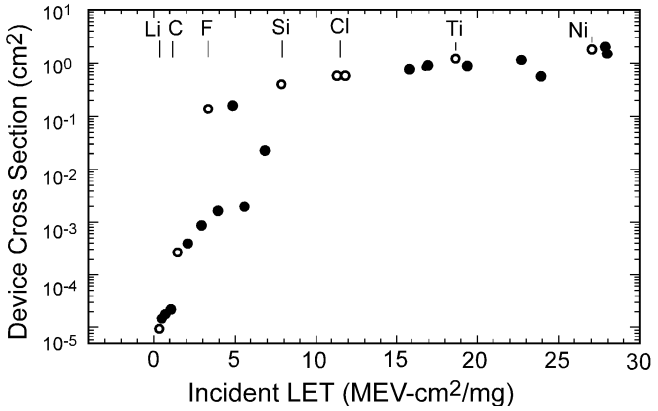

Fig. 2. The cross section data for the Oki DRAM does not follow the "effective LET" model very well. Note the statistical error bars are smaller than the size of the plotting symbols. Also, hollow symbols are normal incident ions.

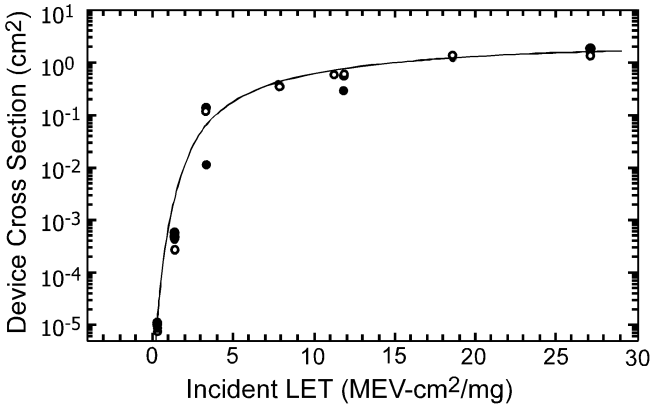

Fig. 3. Cross section vs. azimuthal angle for the 64Mb Toshiba DRAM irradiated with 141MeV fluorine at a 48° tilt angle presented in polar coordinates. Error bars are 10% or better.

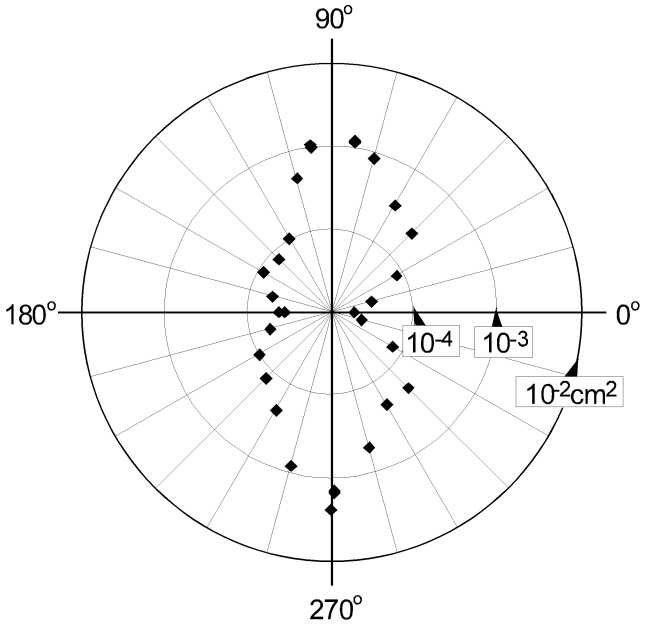

Fig. 4. For this choice of azimuthal angle, cross section vs. effective LET looks good, but this is an illusion that will lead to an order of magnitude high SEU rate calculation. (Error bars are less than 10%).

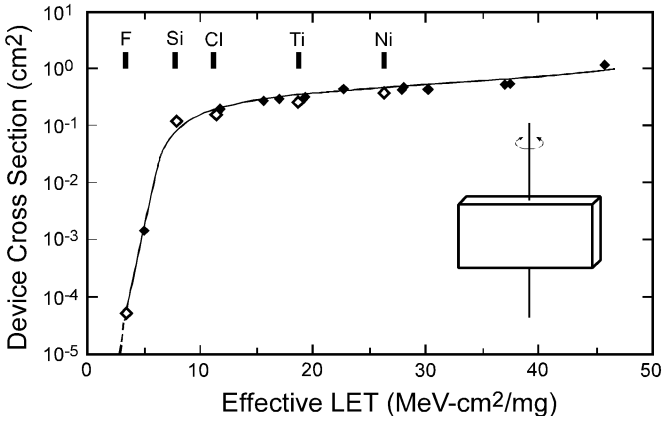

Fig. 5. This alternate choice of azimuthal angle yields a messy cross section vs. effective LET, signaling a tilt-angle dependence problem, but still allowing one to miss the strong azimuthal dependence.

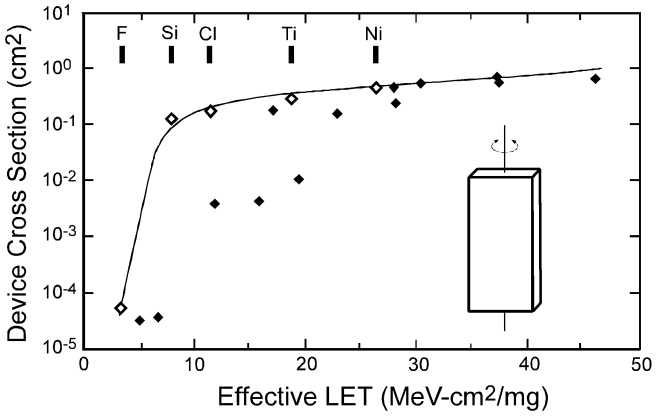

Fig. 6. An isotropic model of the Oki response at different tilt angles yields a much better fit.

Rate Calculation Method	Results
Cosine Law to 85°	21
Usual RPP (A=5)	15
Cube RPP	5.5
Isotropic	5.3

TABLE I
COMPARISON OF CALCULATED OKI RATES (ERRORS PER DEVICE-DAY)